INNOVARE JOURNAL OF SCIENCES
Vol 8, Special Issue 1, 2020
ISSN-2321-5496

Full Proceeding Paper

"STRUCTURAL PROPERTIES OF HOLMIUM DOPED COBALT FERRITE BY STANDARD CERAMIC TECHNIQUE"

P. K. GAIKWAD, S.S. SAWANT*

Department of Physics, Shri Chhatrapati Shivaji College, Omerga (M.S.) India. Email : drsawantss@gmail.com

Received: 25 January 2020, Revised and Accepted: 17 March 2020

ABSTRACT

Objective: Compositions of $CoHo_xFe_{2-x}O_4$ (x = 0.00 and 0.02) was prepared by standard ceramic technique using AR grade CoO_2, Ho_2O_3 and Fe_2O_3. The samples were characterized by X-ray diffraction technique and the analysis of XRD patterns reveals the formation of single phase cubic spinel structure. The structural parameters like lattice constant (a), x- ray density(d_x), bulk density (d_B), particle size (t) and porosity (P), tetrahedral and octahedral bondlength (d_{AX} and d_{BX}), the tetrahedral edge (d_{AXE}), and the shared and unshared octahedral edge (d_{BEX} and d_{BXEU}) can be calculated were calculated form XRD data and effect of Ho^{3+} doped cobalt ferrite was studied. Thus, the rare earth Ho^{3+} doped cobalt ferrite strongly influences the physical properties of cobalt ferrite.

Materials and Methods: Present series was prepared by standard ceramic technique using AR grade CoO_2, Ho_2O_3 and Fe_2O_3.

Results: The XRD pattern shows that both the samples possess single phase cubic spinel structure. No extra peak of Ho^{3+} is observed for x =0.02 sample. Lattice constant, X-ray density of Ho^{3+} doped cobalt ferrite is increases than that of pure cobalt ferrite.

Conclusion: The rare earth Ho^{3+} doped cobalt ferrite strongly influences the physical properties of cobalt ferrite.

Keywords: Cobalt ferrite, Rare earth, Structural properties.

INTRODUCTION

The most important advantage of ferrites is their degree of compositional variability. Most of the original intrinsic properties on ferrites are made on the spinel ferrites such as MFe_2O_4 (M is a divalent metal ion Mn, Co and Ni) are used in the fabrication of multilayer chip inductor and surface mount devices in electronic products such as cellular phones, digital diaries, video camera, recorder and floppy devices. Which have high resistivity and low eddy current losses are used as inductor, memory cores, high frequency transformers and recording heads. The important electrical and magnetic properties of ferrite depend on chemical compositions, method of preparation and cation distribution [1-2].

In the family of spinel ferrites cobalt ferrite ($CoFe_2O_4$) is a unique ferrite having inverse spinel structure. Cobalt ferrite have regarded as one of the competitive candidates for high density magnetic recording media because of their moderate saturation magnetization, high coericivity, mechanical hardness and chemical stability. Cobalt ferrites are among the most widely used magnetic materials having low cost, high performance for high frequency applications [3-4]. It has a hard magnetic material possessing high magneto crystalline anisotropy, high Curie temperature, high corecivity and moderate saturation magnetization along with the chemical stability and mechanical hardness [5]. Several researchers have studied pure and substituted cobalt ferrite with a view to understand their basic properties [6].

Recent research shows by introducing rare earth ions into the spinel lattice, can lead to small changes in the structural, magnetization and Curie temperature of the spinel ferrite. A. A. Sattar et al. [7] has studied the role of rare earth doped in the mixed polycrystalline Mn-Zn ferrite. Jing Jiang et al. [8] reported the role of Sm^{3+} substitution in magnetic properties of Zn–Cu–Cr spinel ferrites. The influence of the doped of Gd^{3+} of the structural and electrical conductivity of nickel ferrite has been reported by Said [9] and the doped of Y^{3+} of the structural, electrical and dielectric properties of conductivity of nickel ferrite has been reported by M. Ishaque [10] both have found that the lattice constant increases with doped rare earth contents. Many researchers [11-15] have studied the role of rare earth doped in the pure $CoFe_2O_4$ matrix but to the best of our knowledge no systematic report is available in the literature showing the effect of Ho^{3+} ions in the pure $CoFe_2O_4$ matrix.

The aim of the present work is to investigate the effect of rare earth Ho^{3+} doping on the structural and magnetic properties of cobalt ferrite synthesized by standard ceramic technique.

EXPERIMENTAL DETAILS

Polycrystalline specimens of $CoHo_xFe_{2-x}O_4$ (x = 0.00 and 0.02) were prepared by standard ceramic technique [16] using analytical reagent grade oxides (99.99%) of CoO, Fe_2O_3 and Ho_2O_3. Compounds were accurately weighted in molecular weight percentage with single pan microbalance and mixed powders were wet ground and pre-sintered at 950^0 C for 24 hours. The sintered powder is again re-ground and pelletized. Polyvinyl alcohol was used as a binder in making circular pellets of 10mm diameter and 2–3mm thickness. The pellets were finally sintered in muffle furnace for 1180^0 C for 24 hours and then slowly cooled to the room temperature. X-Ray diffraction patterns were taken at room temperature to confirm the crystal structure of the prepared samples. The XRD patterns were recorded in the 2θ range from 20^0 to 80^0 using Cu-kα radiation (λ = 1.5406 Å) with scanning rate 2^0 per/m [17, 18].

RESULT AND DISCUSSION

Structural analysis

Figure 1 represents the X-ray diffraction pattern (XRD) of pure (x=0.00) and Ho^{3+} doped cobalt ferrite ($CoHo_xFe_{2-x}O_4$ with x = 0.02) recorded at room temperature and 2θ range 20^0-80^0. It is evident from XRD pattern that both the samples (x= 0.0 and 0.02) possesses single phase cubic spinel structure. No extra peak of Ho^{3+} is observed for x =0.02 sample. It is observed that the pure $CoFe_2O_4$ (x=0.00) shows the spinel phase matched with standard pattern (ICSD00-001-1121) [19]. Similar reports of XRD pattern are available in the literature [20-25].

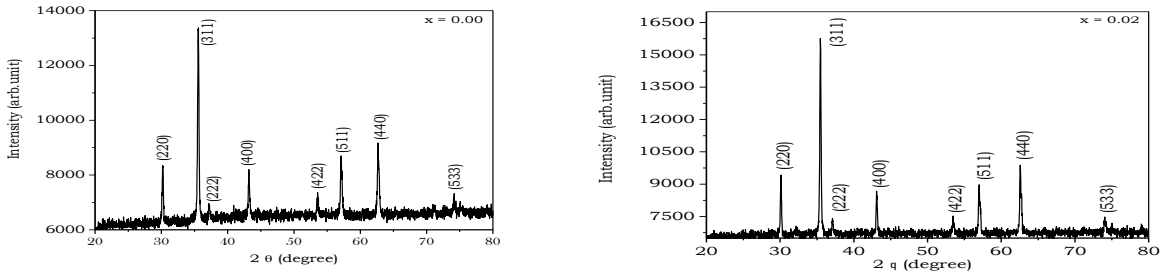

Fig. 1: XRD patterns of $CoHo_xFe_{2-x}O_4$.

Using XRD data the lattice constant (a) was calculated using standard relation [26, 27] for cubic spinel structure. Fig 2 shows that the values of lattice constant are given increases than that of pure cobalt ferrite. This observed behavior of lattice constant is attributed to the large difference between ionic radii of Fe^{3+} (0.645 Å) and Ho^{3+} (1.04 Å). The replacement of Fe^{3+} ions by Ho^{3+} ions causes the increase in lattice constant of Ho^{3+} doped cobalt ferrite. Our results on lattice constant are in full agreement with those reported in the literature [26, 27].

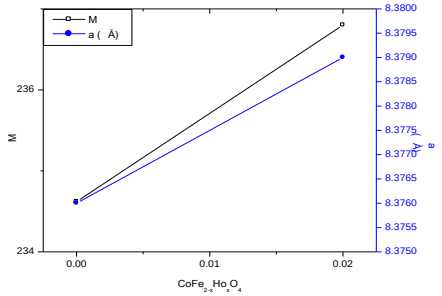

Fig. 2 : Molecular weight (M) and Lattice constant (a) of $CoFe_{2-x}Ho_xO_4$ system.

The X-ray density (d_x) was calculated from the XRD data using the relation discussed elsewhere [28]. The X-ray density (d_x) was calculated using the equation.

$$d_x = \frac{ZM}{N_a a^3} \qquad \text{....(1)}$$

Where 'Z' is number of molecules per unit cell. (For spinel system Z= 8), 'M' is the molar mass of the ferrite, 'N_a' is the Avogadro's number and 'a^3' is the unit cell volume computed from the values of lattice constant. X-ray density (dx) increases almost linearly with the Ho^{3+} doped because the Fe^{3+} ions on the octahedral sites are being replaced by the larger mass Ho^{3+} doped ions. Fig 3 shows that the bulk density of the samples was measured by using Archimedes principle.

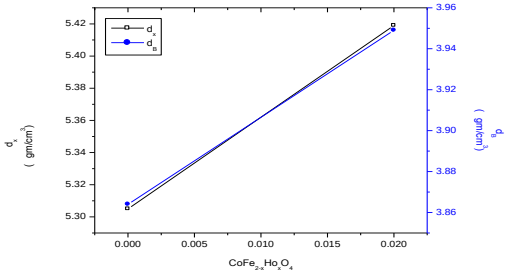

Fig 3: X- ray density (dx) and bulk density (d_B) of $CoFe_{2-x}Ho_xO_4$ system.

The porosity of the samples was calculated by using the following relation and values are tabulated in Table 1.

$$p = \left(1 - \frac{d_B}{d_x}\right) \times 100\% \qquad \text{...(2)}$$

where d_B is the bulk density and d_x is X-ray density. The particle size 't' of each sample was determined by considering full width at half maximum (FWHM) of most intense peak (311) by using Scherer formula [30] and values are given in Table 1. It is observed that Table 1 that the particle size pure and Ho^{3+} doped cobalt ferrite is almost same and is in micrometer range.

The particle size't' of sample was determined by most intense peak (311) by using the relation

$$t = \frac{0.9\lambda}{\beta \cos\theta} \qquad \textbf{...(3)}$$

Where β the full width at half maximum (FWHM) and λ is wavelength of the target material. The particle size values are given in Fig 4. It is observed that the particle size of Ho^{3+} doped is smaller than $CoFe_2O_4$.

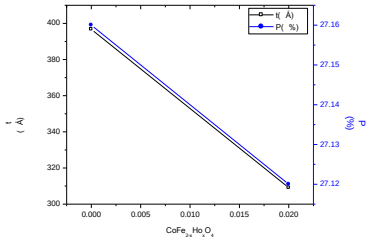

Fig 4: Particle size (t) and Porosity (P) of $CoFe_{2-x}Ho_xO_4$ system.

Fig 5: shows that the values of the tetrahedral and octahedral bondlength (d_{AX} and d_{BX}),

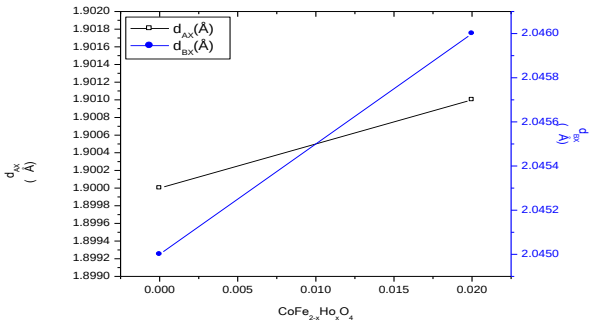

Fig. 5: Tetrahedral bond (d_{AX}) and octahedral bond (d_{BX}) of $CoFe_{2-x}Ho_xO_4$ system.

The tetrahedral edge (d_{AXE}), and the shared and unshared octahedral edge (d_{BEX} and d_{BXEU}) can be calculated according Eqs (4) ~ (8). Using the value of the lattice parameter 'a' (Å) and the oxygen position parameter 'u' (u=0.381 Å).

Table 2: Tetra edge (d_{AXE}) and octa edge (d_{BXC}) of $CoFe_{2-x}Ho_xO_4$ system.

$CoFe_{2-x}Ho_xO_4$	d_{AXE} (Å)	d_{BXE} (Å)	
		(Shared)	(Unshared)
x=0.00	3.103	2.819	2.963
x=0.02	3.105	2.820	2.964

The value of the bondlength of the tetrahedral and octahedral sites are shown in Table 2, It is seen that the all values are depend on the lattice parameter so, the lattice parameter increases, then the edge and the bondlength of the tetrahedral and octahedral sites are increases.

$$d_{AX} = a\sqrt{3}\left(u - \frac{1}{4}\right) \quad \text{...(4)}$$

$$d_{BX} = a\left[3u^2 - \left(\frac{11}{4}\right)u + \left(\frac{43}{64}\right)\right]^{\frac{1}{2}} \quad \text{...(5)}$$

$$d_{AXE} = a\sqrt{2}\left(2u - \frac{1}{2}\right) \quad \text{...(6)}$$

$$d_{BAX} = a\sqrt{2}(1-2u) \quad \text{...(7)}$$

$$d_{BXEU} = a\left[4u^2 - 3u + \left(\frac{11}{16}\right)\right]^{\frac{1}{2}} \quad \text{...(8)}$$

The distance between magnetic ions (hopping length) in the tetrahedral sites is given by Eqs (9) ~(10).

$$L_A = \frac{a\sqrt{3}}{4} \quad \text{....(9)}$$

$$L_B = \frac{a\sqrt{2}}{4} \quad \text{....(10)}$$

where 'a' is the lattice constant, the value Hopping length (L_A, L_B) are shown in Fig 6, Hopping length (L_A, L_B) values are depend on the lattice parameter so, the lattice parameter increases so the Hopping length (L_A, L_B) also increases.

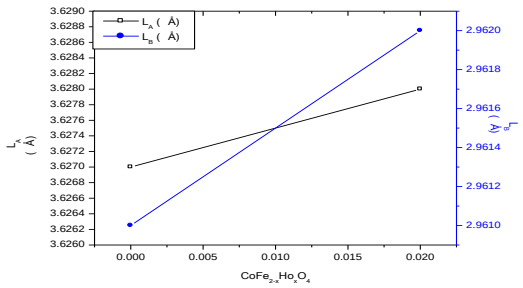

Fig 6: Hopping length (L_A, L_B) of $CoFe_{2-x}Ho_xO_4$ system.

CONCLUSION

Compositions of $CoHo_xFe_{2-x}O_4$ (x = 0.00 and 0.02) was prepared by standard ceramic technique. The XRD pattern that both the samples possesses single phase cubic spinel structure. No extra peak of Ho^{3+} is observed for x =0.02 sample. Lattice constant, X-ray density of Ho^{3+} doped cobalt ferrite is increases than that of pure cobalt ferrite. The values of the tetrahedral and octahedral bondlength, the tetrahedral edge, and the shared and unshared octahedral edge, Hopping length (L_A, L_B) values are depend on the lattice parameter so, the lattice parameter increases so the all these values are also increases.

REFERENCES:

a. A. M. Abo E1 Ata, M. K. E1 Nimir, S. M. Attia, D. E1 Kony and A. H. A1-Hammadi. J. Magn. Magn. Mater. 297 (2006) 33.
2. X. Lu, G. Liang, Q. Sun, C. Yang. J. Mater. Let. 65 (2011) 674.
3. P. K. Gaikwad, V. S. Shinde and S. S. Sawant, Int. Res. J. of Science and Engineering. Special Issue A5: XX-XX (2018)1-4.
4. P. K. Gaikwad, Int. J. of Eng. and Adv. Dev. Vol-4 Jan (2018) 58-63.
5. B.G. Toksha, S.E. Shirsath, S.M. Patange and K.M. Jadhav. Solid State Commun. 147 (2008) 479.
6. Ying Zhang and Dijiang Wen. Mater. Sci. Eng. B. 172 (2010) 331.
7. A. A. Sattar and A. M. Samy. J. Mater. Sci. 37 (2002) 4499.
8. Mansor Al-Haj. J. Magn. Magn. Mater 299(2006) 435.
9. M. Z. Said. Mater. Lett. 34 (1998) 305.
10. M. Ishaque, M. U. Islam, M. A. Khan, I. Z. Rahman, A. Genson and S. Hampshire.Physica B 405 (2010) 1532.
11. I. P. Muthuselvan and R. N. Bhowmik. J. Magn. Magn. Mater. 322 (2010) 767.
12. J. Peng, M. Hojamberdiv, Y. Xu, B. Cao, J. Wang and H. Wu.J. Magn. Magn. Mater. 323 (2011) 133.
13. M. L. Kahn and Z. H. Zhang. Appl. Phys. Lett. 78 (2001).
14. L. Zhao, H. Yang and L. Lu. J. Mater. Sci.19 (2008) 992.
15. L. Zhao, H. Yang, X. Zhao, L. Cui and S. Feng. Mater. Lett. 60 (2006) 1.
16. C. N. Rao "Chemical approaches to the synthesis of inorganic materials"Wiley, New York (1994)
17. P. K. Gaikwad, S. S. Sawant and K. M. Jadhav, J. Adv. App. Sci. Tech. Vol. 1 Issue 2 Dec (2014) 35-37.
18. S. Jie, W. Lixi, Xu Naicen and Z. Qitu.J. Rare Earths 28 (2010) 451.
19. I. Ali, M. U. Islam, M. Ishaque, H. M. Khan, M. N. Ashiq, M. U. Rana J. Mag. Mag. Mat. 324 (2012) 3773–3777
20. P. K. Gaikwad, S. S. Sawant, G. B. Jadhav and K. M. Jadhav, Golden Res. Thoughts Vol. 2 Issue 7 Jan (2013) 8-13.
21. J. Jiang, Y. Yang and L. Li. Physica B. 399 (2007) 105.
22. P. K. Roy, B. B. Nayak and J. Bera.J. Magn. Magn. Mater 320 (2008) 1128.
23. T. J. Shinde, A. B. Gadkari and P. N. Yasambekar.J. Mater. Sci. Mater Electron 21 (2010) 120.
24. Y. Yanmin, J. Jing, L. Liangchao and X. Yanlong. J. Rare Earths 25 (2007) 228.
25. J. Jiang, L. Li, F. Xu and Y. Xie.Mater. Sci. Eng. B. 137 (2007) 166.
26. K. K. Bharathi, J. A. Chelvane and G. Markandeyulu. J. Magn. Magn. Mater 321 (2009) 3677.
27. B. D. Cullity, "Elements of X-ray diffraction" Addison –Wesley Pub. Com. Inc (1956)
28. M. A. Ahmed, E, Ateia, S.I. E1-Dek.Mater. Letts 57(2003) 4256.
29. P. K. Roy, J. Bera. Mater. Res. Bull. 42 (2007) 77
30. J. Jiang, Y. M. Yang and L. C. Li Physica B 399 (2010) 451.